Nucleic Acids Research, 1995, Vol. 23, No. 16 3141–3151

Assembly, nuclear import and function of U7 snRNPs studied by microinjection of synthetic U7 RNA into *Xenopus* oocytes

Branko Stefanovic+, Wolfgang Hackl[1], Reinhard Lührmann[1] and Daniel Schümperli*

Abteilung für Entwicklungsbiologie, Zoologisches Institut der Universität Bern, 3012 Bern, Switzerland and [1]Institut für Molekularbiologie und Tumorforschung, Philipps-Universität, 35037 Marburg, Germany

Received May 30, 1995; Revised and Accepted July 10, 1995

ABSTRACT

In *Xenopus* oocytes *in vitro* transcribed mouse U7 RNA is assembled into small nuclear ribonucleoproteins (snRNPs) that are functional in histone RNA 3′ processing. If the special Sm binding site of U7 (AAUUUGUCUAG, U7 Sm WT) is converted into the canonical Sm sequence derived from the major snRNAs (AAUUUUUGGAG, U7 Sm OPT) the RNA assembles into a particle which accumulates more efficiently in the nucleus, but which is non-functional. U7 RNA with a heavily mutated Sm binding site (AACGCGUCAUG, U7 Sm MUT) is deficient in nuclear accumulation and function. By UV cross-linking U7 Sm WT RNA can be linked to three proteins, i.e. the common snRNP proteins G and B/B′ and an apparently U7-specific protein of 40 kDa. As a result of altering the Sm binding site, U7 Sm OPT RNA cannot be cross-linked to the 40 kDa protein and no cross-links are obtained with U7 Sm MUT RNA. The fact that the Sm site also interacts with at least one U7-specific protein is so far unique to U7 RNA and may provide an explanation for the atypical sequence of this site. All described RNA–protein interactions, including that with the 40 kDa protein, already occur in the cytoplasm. An additional cytoplasmic photoadduct obtained with U7 Sm WT and U7 Sm OPT, but not U7 Sm MUT, RNAs is indicative of a protein of 60–80 kDa. The m7G cap structure of U7 Sm WT and U7 Sm OPT RNA becomes hypermethylated. However, the 3mG cap enhances, but is not required for, nuclear accumulation. Finally, U7 Sm WT RNA is functional in histone RNA processing even when bearing an ApppG cap.

INTRODUCTION

U7 RNA was initially discovered as a short RNA of sea urchins that can complement deficient RNA 3′ processing of a sea urchin histone *H3* gene microinjected into *Xenopus* oocytes (1). Later it was shown that U7 RNA in nuclear extracts is partly resistant to micrococcal nuclease digestion (2) and immunoprecipitable with antibodies directed against Sm proteins or the trimethylguanosine (3mG) cap structure of U snRNAs (3), suggesting that it is assembled into a small nuclear ribonucleoprotein (snRNP) *in vivo*. Purification of mouse U7 snRNP (4) confirmed its association with the entire set of common Sm proteins (5) and with two additional, apparently U7 snRNP-specific, proteins of 50 and 14 kDa. U7 is a minor snRNP present at ~10^3–10^4 copies in mammalian cells (6), as compared with 2×10^5–10^6 copies for spliceosomal snRNPs (7). With respect to its role in 3′-end formation of replication-dependent histone pre-mRNA, there is genetic (8,9) and biochemical evidence (10) that the particle acts through base pairing between the 5′-end of U7 RNA and the spacer element of histone pre-mRNA (for a review see 11).

The known U7 RNAs of various species (12–16) are 58–62 nucleotides (nt) long and can be folded into a simple secondary structure with the 3′ half forming a long stem–loop. This stem–loop is conserved as a structure, but not as a sequence. All U7 RNAs are complementary at their 5′-ends to the spacer elements of their cognate histone pre-mRNAs, this base pairing potential being absolutely required for histone RNA processing. Moreover, U7 RNA contains the sequence $^{AA}_{UG}$UUU$^{G}_{C}$UCUAG, located between the 5′ base pairing region and the 3′-terminal stem–loop, which is functionally equivalent to the so-called Sm binding site of major snRNAs, PuAUUUUUGPu (2), however, the sequence similarity is restricted to the 5′ portion of this element.

Previous work from our laboratory pointed to the significance of this special Sm binding site for the low levels of U7 RNA accumulating in cell nuclei (6). Wild-type mouse U7 RNA accumulated in the nucleus of transiently tranfected HeLa cells at a 2–4-fold lower level than a mouse U1 RNA. When the U7-specific Sm binding site (U7 Sm WT) was changed into the canonical Sm sequence, AAUUUUUGG, derived from the major snRNAs (U7 Sm OPT; Fig. 1) nuclear accumulation and precipitability with anti-Sm antibodies paralleled that of U1 RNA. Apparently the U7 Sm WT site promotes inefficient

* To whom correspondence should be addressed

+Present address. Division of Digestive Diseases, Department of Medicine, University of North Carolina, CB# 7080, Burnett-Womack Building, Chapel Hill, NC 27599-7080, USA

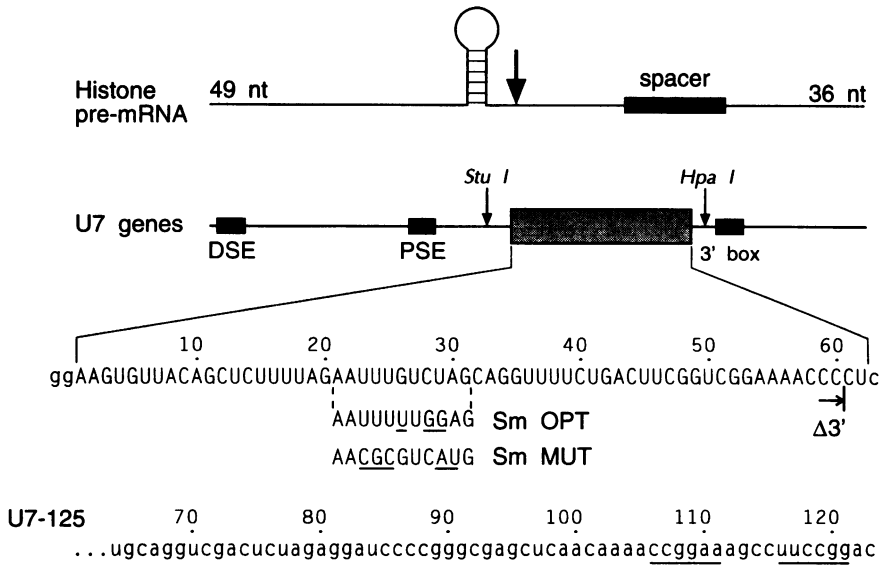

Figure 1. Constructs used for microinjections. (**Top**) Structure of 85 nt long histone pre-mRNA containing the hairpin–loop and spacer elements of the mouse histone *H4-12* gene (12/12 RNA; 10,19). The vertical arrow indicates the processing site. (**Middle**) Schematic representation of the mouse *U7* gene (6,14). The proximal (PSE) and distal (DSE) sequence elements of the promoter and the 3′ box are shown as black boxes. (**Bottom**) Sequence of U7 Sm WT RNA and of specific mutants used in this work. The nucleotide sequence of mouse U7 RNA (22) is shown in upper case, additional nucleotides present in the *in vitro* transcripts in lower case. Numbering starts with the first nucleotide of mouse U7 RNA. For mutants U7 Sm OPT and U7 Sm MUT only the relevant portion of the sequence is shown and altered nucleotides are underlined. Δ3′ indicates the end of the shorter U7 SM WT and U7 Sm OPT transcripts used in Figure 6, to which an additional pCp was added for 3′-end-labelling. For U7-125 used in Figure 3C the complementary nucleotides of the 3′-terminal stem–loop are underlined.

assembly with Sm proteins, resulting in the majority of synthesized U7 RNA remaining free and being either rapidly degraded (in HeLa cells) or retained in the cytoplasm (in *Xenopus* oocytes; 6). Together with the low copy number of *U7* genes (14,15), this phenomenon can fully account for U7 being a minor snRNA.

In the same paper (6) we developed a functional assay based on the injection of mouse *U7* genes into *Xenopus* oocytes. Interestingly, only *U7 Sm WT*, but not *U7 Sm OPT*, was functional in this assay. Here we show that this complementation can also be achieved by injecting *in vitro* synthesized mouse U7 Sm WT RNA, but that U7 Sm OPT RNA is again non-functional. This complementation assay has been used to characterize important parameters for assembly and nuclear import. In addition, we have characterized the structure of functional and non-functional U7 snRNPs by protein–RNA cross-linking.

MATERIALS AND METHODS

Plasmids and *in vitro* transcription

For *in vitro* transcription of U7 Sm WT RNA a double-stranded oligonucleotide containing the mouse *U7* coding region with two additional G residues at the 5′-end was ligated next to the T7 promoter of a Bluescript vector (plasmid OT7 as modified by K. Kälin, Institute for Molecular Biology I, University of Zürich; the resulting plasmid is called OT7U7). Templates for U7 Sm OPT and U7 Sm MUT RNA were derived from OT7U7 by site-directed mutagenesis (17,18). For *in vitro* transcription the constructs were linearized with *Pst*I and the resulting ends made blunt with T4 DNA polymerase. This resulted in an additional C residue at the 3′-end of transcripts, as compared with natural mouse U7 RNA. Two templates for RNAs that lack the last 2 nt of natural mouse U7 RNA (U7 Sm WT Δ3′ and U7 Sm OPT Δ3′) were created by introducing a *Sma*I site at the appropriate position. A template for producing U7 RNA with a 3′ extension was constructed by ligating the *Eco*RI–*Hin*dIII fragment of a histone pre-mRNA template with a mutated stem–loop (B/12; 19) between the *Eco*RI and *Hin*dIII sites of OT7U7 (OT7U7-107). The linker between the U7 and B/12 sequences was then elongated by inserting the *Pst*I–*Sac*I polylinker fragment of pSP65 between the *Pst*I and *Sac*I sites of OT7U7-107 (OT7U7-125). This template was linearized downstream of the mutant stem–loop structure with *Ava*II. Short histone pre-mRNA (12/12 RNA) from the mouse histone *H4-12* gene was prepared as described (10,19). The sequence of each transcription template was confirmed by dideoxy sequencing (20). Sequences of the resulting RNAs are shown in Figure 1.

All *in vitro* transcripts used for microinjections were synthesized in the presence of either m7GpppG (Boehringer) or ApppG (Pharmacia) cap analogues as follows: 1 μg linearized template was incubated in 10 μl 40 mM Tris–HCl, pH 7.5, 6 mM $MgCl_2$, 13 mM DTT, 2 mM spermidine, 0.1 mg/ml bovine serum albumin, 0.5 mM respective cap analogue, 0.1 mM GTP, 0.5 mM each ATP, UTP, CTP, 25 μCi [α-^{32}P]GTP (800 Ci/mmol; New England Nuclear), 40 U RNAsin (Promega) and 5 U SP6 or T7 RNA polymerase (Boehringer or a gift of Dr B. Müller) for 1 h at 37°C. For 3′-end-labelling U7 Sm WT Δ3′ and U7 Sm OPT Δ3′ templates were transcribed without labelled GTP, the RNAs precipitated with ethanol and end-labelled with [α-^{32}P]pCp (New England Nuclear) and T4 RNA ligase (Pharmacia) (21). All labelled transcripts were purified by electrophoresis through a denaturing gel followed by phenol extraction and ethanol precipitation.

Oocyte microinjection

In vitro synthesized, radiolabelled U7 RNAs (~1.5 fmol) were injected in 20 nl water into the vegetative hemisphere (cytoplasm) of *Xenopus* oocytes. The oocytes were incubated overnight or as long as indicated in modified Barth's medium at 18°C before isolation of RNA or nuclear extract. In complementation experiments we first injected intranuclearly 5 ng/oocyte oligonucleotide cA in 20 nl 88 mM NaCl, 10 mM Tris–HCl, pH 7.5. Oligonucleotide cA is complementary to nt 1–16 of *Xenopus* and mouse U7 RNA (16,22) and targets endogenous RNase H to destroy the resident U7 RNAs. After 5 or 24 h incubation, to allow for degradation of the oligonucleotide, *in vitro* synthesized U7 RNA was injected into the ooplasm as above and incubation continued overnight. Finally, 7.5 fmol 12/12 histone pre-mRNA (5000 c.p.m.) in 20 nl water was injected into the nuclei of the same oocytes. After a further 2 h total oocyte RNA was extracted and analysed. About 10–20 oocytes were injected per sample, unless specified otherwise.

RNA analysis and extract preparation

RNA was extracted by homogenizing total oocytes or nuclear and cytosolic fractions (see below) in 100 mM Na acetate, pH 5.0, 5 mM EDTA, 0.5% SDS followed by phenol/chloroform extraction and ethanol precipitation. Processing of injected histone pre-mRNA was analysed by denaturing gel electrophoresis on 8% polyacrylamide–8.3 M urea gels. Endogenous *Xenopus* U7 RNA was analysed by reverse transcription with primer cBX (TGCTAGACAAAATAGTA), complementary to nt 18–33 of *Xenopus* U7 RNA (6).

Nuclear and cytoplasmic fractions were prepared by dissecting the oocytes in 10 mM NaCl, 125 mM KCl, 1 mM KH_2PO_4, 2 mM $NaHCO_3$, 2.5 mM DTT, 0.5 mM PMSF (23). Separated nuclei were centrifuged for 20 s at low speed, the supernatants removed and nuclei homogenized in 1–5 µl/oocyte buffer D (20 mM HEPES–KOH, pH 7.9, 100 mM KCl, 0.2 mM EDTA, 0.5 mM DTT, 0.1 mM PMSF, 20% glycerol; 24). Cytoplasmic and total oocyte extract were prepared by homogenizing oocytes or cytosol in 130 mM NaCl, 34 mM Na phosphate, pH 7.4 (10–20 µl/oocyte), followed by a 1 min centrifugation in an Eppendorf centrifuge and recovery of the clear supernatant.

Photoaffinity cross-linking

Nuclear or cytoplasmic extracts (2 oocyte equivalents, unless specified otherwise) were irradiated at 254 nm for 20 min from a distance of 5 cm with a Hanau Fluotest Universal type 5201 lamp (25). After mixing with an equal volume of SDS loading buffer (50 mM Tris–HCl, pH 6.8, 100 mM DTT, 2% SDS, 0.1% bromphenol blue, 10% glycerol) the extract was boiled for 2 min and resolved on a 10% SDS–polyacrylamide gel (26). For RNase digestion of photoadducts 50 µl nuclear extract (corresponding to 50 nuclei) was prepared from oocytes injected with [α-^{32}P]UTP-labelled synthetic U7 RNA and UV irradiated as above. The extract was boiled for 2 min and digested with 125 U Benzon nuclease (Merck) for 30 min at room temperature and with 20 µg RNase A for 30 min at 45°C prior to loading on a 15% SDS–polyacrylamide gel.

Immunoprecipitation

For precipitation with anti-3mG cap antibody R1131 (28) 6 fmol uninjected U7 RNA capped with m7GpppG or of ApppG- or m7GpppG-capped RNAs re-extracted from injected oocytes were used. Immunoprecipitations were performed as described (6). RNA was extracted from pellet (and supernatant) fractions and analysed on a 6% denaturing polyacrylamide gel.

For immunoprecipitation of individual photoadducts 40 µl rabbit immune serum directed against the C-terminal portion of human protein G (29) or 40 µl non-immune rabbit serum were coupled to 40 µl protein A–Sepharose (Pharmacia). For monoclonal antibodies 80 µl antibody H57 (directed against human B/B′ protein; 30), 12 µg purified Y-12 antibody (27) or 12 µg D5 antibody (directed against strand exchange protein 1 of *Saccharomyces cerevisiae*; a gift of Dr W. -D. Heyer) were coupled to 40 µl protein G–Sepharose (Pharmacia). Oocyte nuclear extract (20 µl) was UV irradiated as above, boiled for 2 min and added to the antibody suspension in 200 µl IPP150 (150 mM NaCl, 10 mM Tris–HCl, pH 8, 0.05% NP-40) supplemented with 0.1 mM PMSF and 0.1 mM leupeptin. After 2 h the beads were washed three times with IPP150 and bound proteins released by adding 40 µl SDS loading buffer and heating to 65°C. Samples were resolved on a 10% SDS–polyacrylamide gel.

Mapping of cross-links

3′-End-labelled U7 RNAs were injected into the cytoplasm of 200 oocytes and incubated overnight. Whole oocytes were homogenized in 4 ml 130 mM KCl, 34 mM Na phosphate, pH 7.4, 0.1 mM PMSF, 0.1 mM leupeptin, centrifuged for 2 min and the supernatant UV irradiated for 20 min in a small Petri dish. Samples were concentrated by lyophilization and resolved on a preparative 10% SDS–polyacrylamide gel. Photoadducts were excised from the gel, eluted overnight into 400 µl 0.3 M NaCl, 0.1% SDS, 0.1 mM EDTA, 10 mM Tris–HCl, pH 7.5, and hydrolysed with 40 µl 0.5 M KOH for 8 min at 42°C. Free RNA was digested identically. After neutralization with 14 µl 1 M acetic acid and ethanol precipitation samples were run on an 8% sequencing gel. RNase T1 digestion was carried out by incubating the 3′-end-labelled RNA with 10 µg tRNA, 0.01 U RNase T1 in 30 µl 10 mM $MgCl_2$ for 2 min at room temperature, followed by phenol/chloroform extraction and ethanol precipitation.

RESULTS

Sm-dependent nuclear import of synthetic U7 RNA

To determine the requirements for nuclear uptake of U7 snRNPs we injected *in vitro* synthesized and m7G-capped U7 RNAs into the ooplasm and, after overnight incubation, analysed the fraction which had entered the nucleus. We injected three RNAs, U7 Sm WT, U7 Sm OPT (with an Sm binding site corresponding to the consensus derived from spliceosomal snRNAs) and U7 Sm MUT (in which the Sm binding site was completely substituted by an unrelated sequence; Fig. 1). The transcripts contain two additional G residues at the 5′-end to allow for efficient transcription with T7 RNA polymerase and an extra C residue at the 3′-end. All three RNAs appear to be stable in the oocyte after prolonged incubation (Fig. 2, lanes T), although U7 Sm WT and U7 Sm MUT RNAs are shortened by 1–2 nt (compare lanes 2 and 5 with lanes 1 and 4) and U7 Sm OPT RNA by 3–4 nt (lanes 7 and 8). U7 Sm WT and U7 Sm OPT RNA accumulate in the nucleus

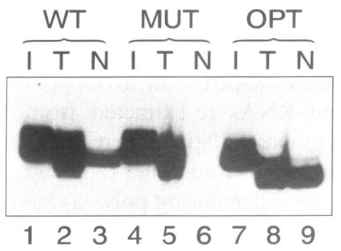

Figure 2. Nuclear uptake of *in vitro* synthesized U7 RNAs is Sm dependent. *In vitro* synthesized radioactively labelled U7 Sm WT (lanes 1–3), U7 Sm MUT (4–6) and U7 Sm OPT (7–9) RNAs were injected into the ooplasm (sequences are as shown in Figure 1, except that the RNAs were synthesized with a 7-methylguanosine cap structure). After 18 h total (T) and nuclear (N) RNA (2 oocyte equivalents) and a similar amount of input RNA (I) were analysed on a denaturing polyacrylamide gel.

(lanes 3 and 9), although the latter does so ~3–4 times more efficiently. U7 Sm MUT RNA does not enter the nucleus (lane 6), suggesting that nuclear import is Sm specific. If the RNAs were injected directly into the nucleus they were exported into the ooplasm within 1 h and re-imported in the same Sm-dependent manner (data not shown). Thus the three variant U7 RNAs, when injected as m7G-capped synthetic transcripts, accumulate in the nucleus in relative amounts similar to when transcribed from an injected gene (6).

The following additional experiments suggest that the injected RNAs accumulate in the nucleus as snRNPs (data not shown): During non-denaturing gel electrophoresis of nuclear extracts from injected oocytes U7 Sm WT and U7 Sm OPT RNA migrate as high molecular weight complexes with similar mobilities as native U7 snRNPs from mouse nuclear extract. Moreover, both particles specifically react with the Y-12 monoclonal anti-Sm antibody (27).

Hypermethylation of the cap structure and its role in nuclear import

Spliceosomal snRNAs undergo a modification of the cap structure from m7G to 3mG in a process that depends on the binding of common Sm proteins (31). We therefore analysed whether *in vitro* synthesized, m7G-capped U7 RNA also acquires a hypermethylated cap. The three RNAs, U7 Sm WT, U7 Sm OPT and U7 Sm MUT, synthesized in the presence of either m7GpppG or ApppG cap analogues, were injected into the oocyte cytoplasm and, after overnight incubation, re-extracted from the oocytes. These samples, together with the original (uninjected) m7G-capped RNAs, were subjected to immunoprecipitation with anti-3mG cap antibody (28). The antibody used in this experiment (R1131) is specific for the 3mG cap structure, since the uninjected m7G-capped RNAs (Fig. 3A, lanes 1, 4 and 7) or the re-extracted ApppG-capped RNAs (lanes 3, 6 and 9) are not precipitated. In contrast, U7 Sm WT (lane 2) and U7 Sm OPT RNA (lane 5), initially m7G-capped and re-extracted after incubation in the oocytes, are precipitated by this antibody. No cap hypermethylation can be detected for U7 Sm MUT RNA (lane 8). It therefore seems that U7 RNA undergoes cap hypermethylation in a Sm-dependent manner.

We next investigated the role of the 3mG cap in nuclear import. We synthesized U7 RNAs with m7GpppG or ApppG cap analogues and analysed their nucleocytoplasmic distribution after cytoplasmic injection and overnight incubation. In contrast to the m7G cap, the ApppG cap cannot be hypermethylated. Nevertheless,

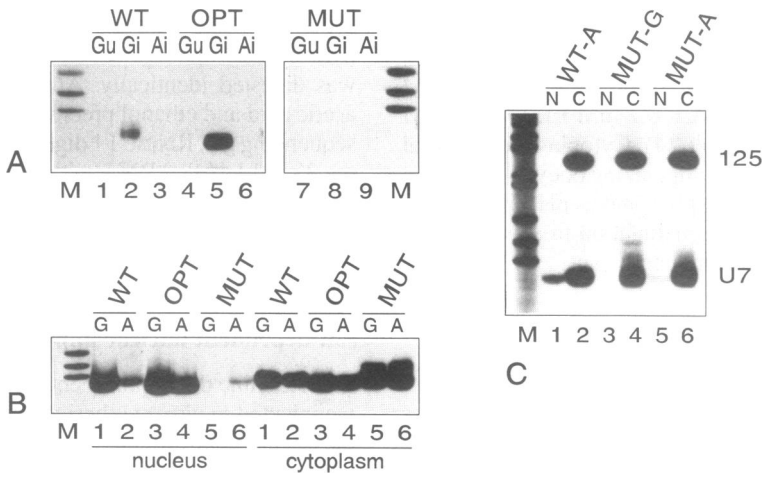

Figure 3. Cap hypermethylation and its effect on nuclear import of U7 RNA. (**A**) Cap hypermethylation of wild-type and mutant U7 RNAs. Radioactively labelled U7 Sm WT (lanes 1–3), U7 Sm OPT (4–6) and U7 Sm MUT RNAs (7–9) were synthesized *in vitro* in the presence of either m7GpppG (lanes Gu and Gi) or ApppG (lanes Ai) cap analogues. These RNAs were injected into the ooplasm and after 18 h total oocyte RNA was subjected to immunoprecipitation with a rabbit anti-3mG cap antibody (lanes Gi and Ai). In lanes Gu uninjected m7G-capped RNA was subjected to immunoprecipitation. Only pellet fractions are shown, but all RNAs were recovered as mostly intact RNA in the supernatant fractions. Lane M, pBR322 cut with *Hpa*II (fragments of 90, 76 and 67 nt are visible). (**B**) The correct cap structure is important, but not required, for nuclear import of U7 RNA. m7GpppG- (lanes G) or ApppG-capped (lanes A) U7 Sm WT (lanes 1 and 2), U7 Sm OPT (lanes 3 and 4) and U7 Sm MUT RNAs (lanes 5 and 6) were injected into the ooplasm. After 18 h nuclear and cytoplasmic RNAs were analysed on a denaturing polyacrylamide gel. Lane M, size marker; see (A). (**C**) Low levels of ApppG-capped U7 Sm WT and U7 Sm MUT RNAs are found in the nucleus. ApppG-capped U7 Sm WT (lanes WT-A) and m7GpppG-capped (lanes MUT-G) and ApppG-capped (lanes MUT-A) U7 Sm MUT RNA were co-injected together with m7GpppG-capped U7-125 RNA (see Fig. 1) into the ooplasm. After 18 h nuclear (lanes N) and cytoplasmic (lanes C) RNAs were analysed on a denaturing polyacrylamide gel. U7-125 does not enter the nucleus and serves as a cytoplasmic marker. Lane M, pBR322 cut with *Hpa*II (fragments of 217, 201, 160, 147, 122, 110, 90, 76 and 67 nt are visible). All lanes correspond to 4 oocyte equivalents, except for A7–A9 (10 oocyte equivalents).

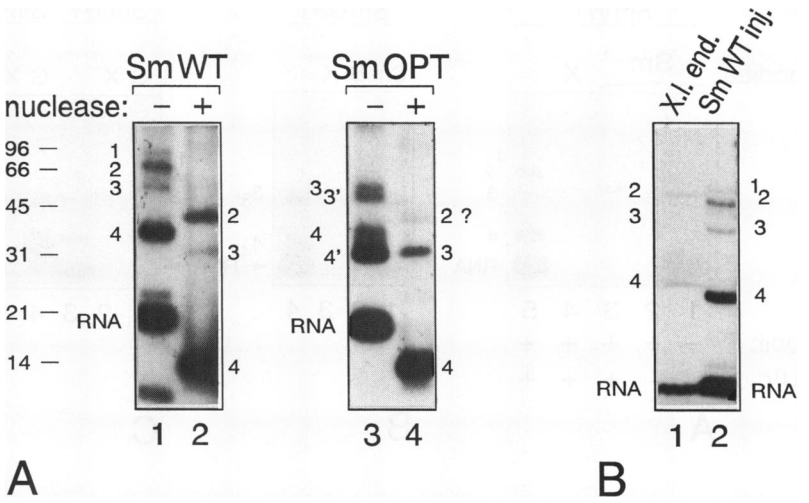

Figure 4. Structural analysis of U7 snRNPs by UV cross-linking. (**A**) Nuclear extract from oocytes having received a cytoplasmic injection of *in vitro* synthesized U7 Sm WT (lanes 1 and 2) or U7 Sm OPT RNA (lanes 3 and 4) was UV irradiated. The samples were resolved on a 15% polyacrylamide–SDS gel either without (lanes 1 and 3, 5 oocyte equivalents) or after digestion with Benzon nuclease and RNase A (lanes 2 and 4, 50 oocyte equivalents). Numbers on the left indicate the molecular weights in kDa and the migration of Coomassie stained marker proteins. To increase recovery of radioactivity after nuclease digestion the injected U7 RNAs were labelled with [α-^{32}P]UTP; in all other figures except Figure 6 they were labelled with [α-^{32}P]GTP. Lanes 1 and 2 are from a longer exposure and represent adjacent lanes to lanes 3 and 4. The adducts are labelled 1–4 for U7 Sm WT and 3-3′ and 4-4′ for U7 Sm OPT RNA. The position of free RNA is indicated. For the band in lane 4 labelled 2? see text. (**B**) Comparison of protein–RNA adducts obtained after injection of radiolabelled mouse U7 Sm WT RNA into *Xenopus laevis* oocytes (lane 2, 2 oocyte equivalents) with the pattern observed for *Xenopus* U7 snRNPs (lane 1, 5 oocyte equivalents). In the latter case the content of U7 snRNPs in the oocytes was increased by injection of a clone encoding three *Xenopus U7* genes (16, A. Gruber and D. Schümperli, unpublished results). After 24 h nuclear extract was prepared and U7 RNA was detected by hybridization and co-electrophoresis of radiolabelled oligonucleotide cA complementary to nucleotides 1–16 of U7 RNA (25). Identical, but fainter, bands were obtained when the analysis was performed with uninjected oocytes (data not shown). Electrophoresis was on a 10% polyacrylamide–SDS gel.

ApppG-capped U7 Sm WT RNA accumulates in the nucleus (Fig. 3B, lane 2), albeit less efficiently than with a m7G (3mG) cap (lane 1). Both RNAs associate equally well with Sm proteins, as judged by immunoprecipitation with Y-12 antibody, and the resulting RNP complexes show equal electrophoretic mobility in native gels (data not shown). Therefore, it appears that the reduced nuclear import of ApppG-capped U7 Sm WT RNA is due to the different cap structure itself and not to reduced RNP assembly. This further implies that cap hypermethylation is an important, but not a required, feature for nuclear accumulation of U7 snRNPs in *Xenopus* oocytes. For nuclear import of U7 Sm OPT RNA the proper 3mG cap structure appears to be even less important (Fig. 3B, lanes 3 and 4). Interestingly, for U7 Sm MUT RNA, which is deficient for snRNP assembly and nuclear import when transcribed with a m7G cap (lane 5 and Fig. 2), a small but significant portion is found in the nucleus if the RNA contains an ApppG cap (lane 6; see Fig. 3C and Discussion). It should also be mentioned that the fraction of m7G(3mG)-capped U7 Sm WT RNA entering the nucleus was higher in this experiment than the usual 10–30% (see Fig. 2). The reasons for this difference are unknown; in particular, the amount of RNA injected per oocyte can not have been lower than usual by >1/3. Nevertheless, U7 Sm WT RNA is still imported less efficiently than U7 Sm OPT RNA.

To exclude the possibility that the weak bands seen in lanes 2 and 6 are the result of cytoplasmic contamination we co-injected ApppG-capped U7 Sm WT RNA and m7G- or ApppG-capped U7 Sm MUT RNA together with a longer control RNA that does not enter the nucleus and that serves as a cytoplasmic marker. U7-125 RNA (Fig. 1), a derivative of U7 Sm WT RNA extended for 60 nt at the 3′-end and ending in a stem–loop sequence corresponding to a strongly mutated histone mRNA 3′-end, is completely deficient in nuclear import (Fig. 3C, compare lanes C and N). Despite the fact that U7-125 RNA is not detectable in any nuclear fractions, but in agreement with the data presented in Fig. 3B, co-injected ApppG-capped U7 Sm WT (Fig. 3C, lane 1) and U7 Sm MUT RNAs (lane 5) are found in the nucleus. Again, m7G-capped U7 Sm MUT RNA fails to accumulate in the nucleus (lane 3).

Structural analysis of assembled U7 snRNPs by UV cross-linking

To analyse the structure of the assembled U7 snRNPs we investigated RNA–protein interactions by photoaffinity cross-linking (25,29). Nuclear extract was prepared from oocytes injected with the radiolabelled RNAs, irradiated with UV light and then analysed by SDS–PAGE either without or after digestion with an RNase mixture (see Materials and Methods). By this approach proteins that are in close association with the RNA can be visualized by the transfer of label.

In the absence of RNase digestion four cross-linking adducts are observed with U7 Sm WT RNA (labelled 1–4 in Fig. 4A, lane 1), which decrease in intensity from 4 > 2 > 3 > 1. The very weak adduct 1 cannot be detected in all experiments and is also not detectable after nuclease digestion (lane 2). The molecular weights of the other adducts were estimated after nuclease digestion (which removes all but a small fragment of the RNA) to be 40 [2], 30 [3] and 10 kDa [4] respectively. A direct comparison of the cross-linking products with those obtained with natural *Xenopus* U7 snRNPs is shown in Figure 4B. For this experiment a clone encoding three *Xenopus U7* genes was injected into the oocyte nucleus, the oocytes were incubated

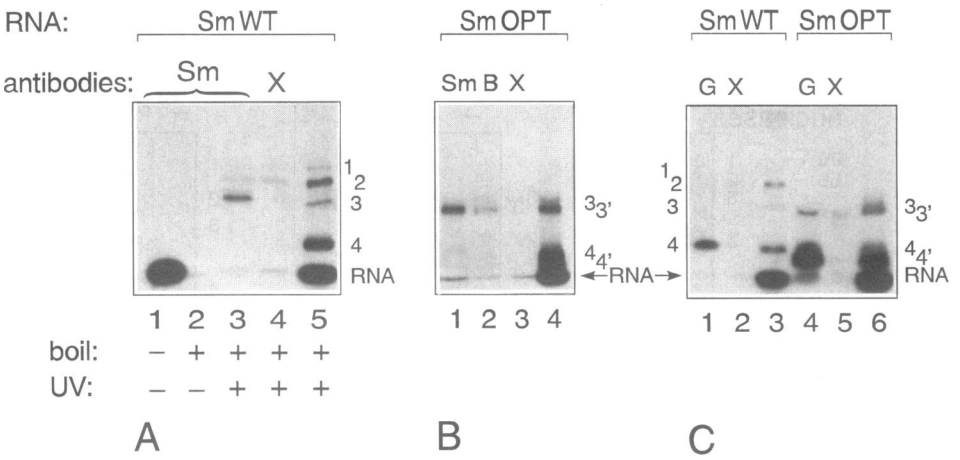

Figure 5. Immunoprecipitation of proteins cross-linked to U7 RNA. (**A** and **B**) Identification of cross-links 3-3′. U7 Sm WT (A) and U7 Sm OPT (B) RNA was injected into *X.laevis* oocytes, UV cross-linking of nuclear extracts was performed (except for lanes A1–2) and samples were boiled (except for lane A1). The samples were separated on 10% polyacrylamide–SDS gels. Lanes A5 and B4, total unprecipitated samples. All other lanes represent pellets of immunoprecipitations: A1–3 and B1, monoclonal anti-Sm antibody Y-12 (Sm); B2, monoclonal antibody H57 directed against human B/B′ protein (B); A4 and B3, control monoclonal antibody D5 (X). The photoadducts are labelled as in Figure 4. Between A4 and A5 two lanes were excised from the photograph. (**C**) Identification of cross-links 4-4′. U7 Sm WT (lanes 1–3) and U7 Sm OPT RNA (lanes 4–6) were analysed as above. All samples were subjected to UV cross-linking and boiling prior to electrophoresis. Lanes 3 and 6, total unprecipitated samples; lanes 1 and 4, immunoprecipitation with rabbit immune serum directed against human protein G (G); lanes 2 and 5, precipitation with rabbit non-immune serum (X). The slight retardation of band 4 in lane 1 versus lane 3 is due to a different electrophoretic behaviour of the precipitated versus unprecipitated samples. All immunoprecipitates correspond to ~10 oocyte equivalents; unprecipitated controls, 3 oocyte equivalents.

overnight and nuclear extract was prepared. Since, in contrast to the *in vitro* transcribed mouse U7 Sm WT RNA (lane 2), the resulting *Xenopus* U7 RNA was not radioactively labelled, it had to be detected by hybridization and subsequent co-electrophoresis of a radioactively labelled oligonucleotide complementary to nt 1–16 of *Xenopus* U7 RNA (lane 1; 25). Due to this method of detection, only a comparison in the absence of nuclease digestion was possible. Moreover, the cross-linking products are slightly retarded on the gel, presumably because of the additional oligonucleotide. Otherwise, the two band patterns are very similar with respect to both the sizes and relative intensities of the bands, except for the very faint adduct 1. It is not possible to say if this adduct is also present in the *Xenopus* sample. Injection of the *Xenopus* genes increased the signal, however, a similar but much fainter band pattern was also obtained if the analysis was performed with nuclear extract from uninjected oocytes (data not shown). As far as this analysis can reveal, the types of UV-induced protein–RNA cross-links formed with U7 Sm WT RNA therefore appear to be identical to those that can be formed within natural *Xenopus* U7 snRNPs.

With U7 Sm OPT RNA no cross-linking products corresponding to bands 1 or 2 of U7 Sm WT RNA are formed (Fig. 4A, lane 3). However, two heterogeneous groups of adducts (3-3′ and 4-4′) are formed, whose upper limits correspond in mobility to bands 3 and 4 obtained with U7 Sm WT RNA. After nuclease digestion each group is reduced to a single band which co-migrates with adducts 3 and 4 of U7 Sm WT RNA (lane 4), suggesting that the multiple bands seen in the undigested sample are due to size heterogeneity in the RNA and not to the cross-linking of a heterogeneous group of proteins. This phenomenon is probably related to the more extensive shortening of the 3′-end of U7 Sm OPT RNA in the oocytes (Fig. 2). In the nuclease-digested sample a faint band with a similar mobility to adduct 2 of U7 Sm WT RNA is also observed. However, bands corresponding to adduct 2 have never been obtained when cross-linking products of U7 Sm OPT RNA were analysed without nuclease digestion (lane 3 and Figs 5 and 7). All bands discussed in this section are sensitive to digestion with proteinase K, indicating that they are due to protein–RNA cross-links (data not shown). No cross-linking products were obtained with U7 Sm MUT RNA, which does not accumulate in the nucleus (see Fig. 7). In contrast, identical cross-linking products were obtained with ApppG-capped as with m7G(3mG)-capped U7 Sm WT RNA (data not shown).

Identity of proteins present in adducts 3 and 4

We suspected that adducts 3 and 4 are formed by the common snRNP proteins B/B′ and G respectively, both because of their apparent sizes (5) and because the G protein has previously been shown to be cross-linked to the Sm binding site in U1 snRNPs (29). Therefore, to identify the proteins present in these adducts nuclear extracts from injected oocytes were UV irradiated as before, the snRNPs were dissociated by boiling and subjected to immunoprecipitation with specific antibodies reacting with individual members of the common snRNP proteins. The Y-12 anti-Sm antibody (27), which recognizes epitopes on the B/B′ and D proteins, can be used to precipitate U7 Sm WT RNA in the absence of cross-linking if a native nuclear extract is used (Fig. 5A, lane 1), but not if the extract has been boiled previously (lane 2), indicating that boiling effectively dissociates the snRNP particles. However, if the extract has been UV irradiated to produce the cross-links and then boiled, the same antibody efficiently precipitates adduct 3 (lane 3). Both Y-12 and an unrelated monoclonal antibody (lane 4) precipitate low amounts of adduct 2, but, most importantly, precipitation of adduct 3 is specific for Y-12. For U7 Sm OPT RNA both Y-12 (Fig. 5B, lane 1) and the H57 antibody specific for the 29 kDa B/B′ proteins (30; lane 2) precipitate adduct 3-3′. No significant precipitation was

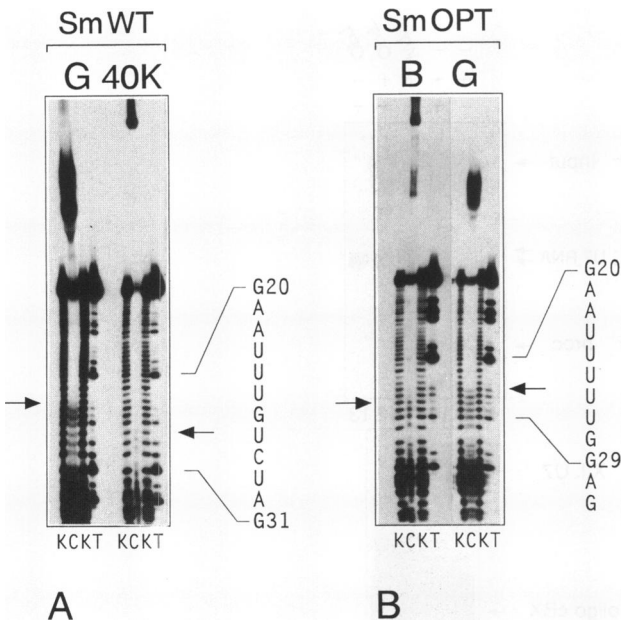

Figure 6. Mapping of cross-links on U7 RNA. 3′-End-labelled U7 Sm WT Δ3′ (**A**) and U7 Sm OPT Δ3′ RNA (**B**) was injected into *X.laevis* oocytes. Whole cell extracts were UV irradiated and the indicated photoadducts were isolated from preparative SDS–polyacrylamide gels. The adducts were subjected to partial KOH hydrolysis and analysed on denaturing polyacrylamide gels (lanes C). Partial KOH ladders (lanes K) and RNase T1 digests (lanes T) of the corresponding input RNAs were run in parallel. The sequences of the relevant portions of the RNAs are shown on the right of each panel. Arrows indicate the largest detectable cleavage products which do not contain the cross-linked proteins. Autoradiography was ~4 times longer for (A) and the left part of (B) than for the right part of (B).

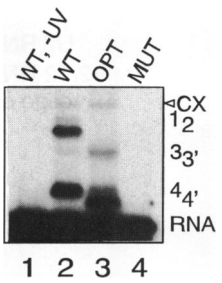

Figure 7. Cytoplasmic assembly of *in vitro* transcribed U7 RNA. Radioactively labelled, m7G-capped U7 Sm WT (lane 2), U7 Sm OPT (lane 3) and U7 Sm MUT (lane 4) RNAs were injected into the ooplasm and after 6 h cytoplasmic extract (4 cytoplasms/sample) was UV irradiated and subjected to electrophoresis on a 10% SDS–polyacrylamide gel. Individual photoadducts are labelled as in Figure 4. Lane 1, U7 Sm WT RNA without UV irradiation of extract. CX and open arrowhead, additional cytoplasmic cross-link.

observed with an unrelated monoclonal antibody (lane 3) or with an antibody specific for the D protein(s), which also carries Sm epitopes (data not shown). A rabbit antiserum specific for the 9 kDa G protein (29) specifically precipitates the lowest adduct, 4, obtained with U7 Sm WT RNA (Fig. 5C, lane 1). For U7 Sm OPT RNA both the G-specific (lane 4) and the control antiserum (lane 5) inefficiently precipitate adduct 3-3′, but, most importantly, only the G-specific serum efficiently precipitates adduct 4-4′. Even though the antibodies used in this study have to react with heterologous (*Xenopus*) proteins, taken together with the apparent sizes of the photoadducts after digestion of the RNA (Fig. 4A) our data strongly suggest that the two smaller proteins cross-linked to U7 RNA in *X.laevis* oocytes correspond to the common B/B′ and G proteins.

Mapping of the sites of protein–RNA cross-linking

To map the cross-links on the RNA we end-labelled the 3′-ends of the injected RNAs with [α-^{32}P]pCp and RNA ligase. Our strategy was to allow assembly of snRNP particles in the oocyte, to form the cross-links by UV irradiation and to purify individual adducts by preparative SDS–PAGE. To reduce the loss of label caused by the observed 3′ trimming activity (Fig. 2) we constructed new transcription templates ending 3 nt further upstream (thus when 3′-end-labelled the RNAs extend beyond the 3′-terminal stem–loop by the sequence CCp, instead of CCU_{OH}, as in *bona fide* mouse U7 RNA). The cross-linking patterns obtained with these RNAs were indistinguishable from those obtained with the longer universally labelled RNAs (data not shown). Moreover, having observed that identical cross-links could also be obtained by irradiating cytoplasmic fractions (see Fig. 7, below), we further increased the yield by UV irradiating total rather than nuclear extracts. Only with these modifications were we able to recover sufficient radioactivity for further analysis from adducts 2 (40 kDa) and 4 (G) of U7 Sm WT and adducts 3 (B/B′) and 4 (G) of U7 Sm OPT RNAs, but not from the very faint adducts 1 or 3 (B/B′) of U7 Sm WT RNA. However, it is possible that, despite the similarity in cross-linking patterns between cytoplasmic and nuclear fractions, the formation of an individual UV adduct may occur at different sites on the RNA, depending on the compartment from which the RNP has been isolated.

Purified adducts were subjected to partial KOH hydrolysis and the products separated by electrophoresis on a sequencing gel (Fig. 6A and B, lanes C), along with original samples of the same RNA treated with either KOH (lanes K) or RNase T1 (lanes T). Although the T1 digestion patterns of the U7 transcripts show some anomalies (e.g. cleavage of U7 Sm WT after U27 instead of G26; for numbering see Fig. 1), the patterns can be properly aligned with the RNA sequence. For U7 Sm WT RNA (Fig. 6A) the largest observable RNA fragment in the KOH-digested material from adduct 4 (G) corresponds to cleavage after U24 or U25. For adduct 2 (40 kDa) the last observed cleavage occurs after C28. For the latter sample the digested cross-linked material shows an anomalous electrophoretic mobility, so that mapping of the cross-link may be in error by not more than 2 nt. Any KOH cleavages located further 5′ result in fragments that are still linked to the corresponding protein and migrate collectively in the upper region of the gel. For U7 Sm OPT RNA (Fig. 6B) the last observable cleavages occur after U25 for adduct 4 (G) and after U27 for adduct 3 (B/B′). Thus in RNP particles present in total oocyte extract all three cross-links occur within a very short stretch of the RNA, i.e. within the natural or altered Sm binding site. Moreover, in the U7 Sm WT particle the cross-link with protein G appears to lie further 5′ than the cross-link with the 40 kDa polypeptide and in U7 Sm OPT particles the cross-link to G precedes the cross-link to B/B′.

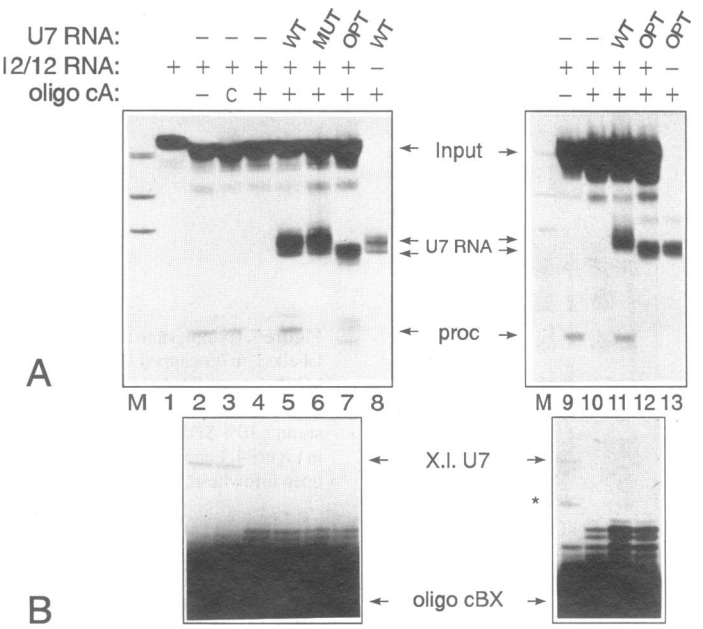

Figure 8. *In vitro* synthesized U7 RNA is active in histone pre-mRNA processing. (**A**) Biochemical complementation of histone pre-mRNA processing with *in vitro* synthesized U7 RNAs. *In vitro* synthesized 7mG-capped mouse U7 RNAs were injected into the cytoplasm of oocytes which had been depleted of endogenous U7 RNAs by targeting with oligonucleotide cA either 5 (left panel) or 24 h previously (right panel). After 18 h incubation 12/12 histone pre-mRNA was injected into the nuclei of the same oocytes. After an additional 2 h total oocyte RNA was extracted and analysed on a denaturing polyacrylamide gel (2 oocyte equivalents/lane). Lane M, pBR322 cut with *Hpa*II (fragments of 90, 76 and 67 nt are visible); lane 1, input histone pre-mRNA; lanes 2 and 9, processing by native oocytes; lane 3, processing by oocytes pre-injected with a control oligonucleotide complementary to nt 10–25 of U1 RNA (c); lanes 4 and 10, (lack of) processing by oocytes depleted of U7 RNA with oligonucleotide cA; lanes 5 and 11, complementation of processing by injection of U7 Sm WT RNA; lane 6, (lack of) complementation with U7 Sm MUT RNA; lanes 7 and 12, (lack of) complementation with U7 Sm OPT RNA; lane 8, as 5, but 12/12 RNA omitted; lane 13, as 12, but 12/12 RNA omitted. Migration of U7 RNAs and of the input and processing product of 12/12 histone pre-mRNA is indicated. The bands in lane 7 of similar size to the processing product are due to degradation of injected U7 Sm OPT RNA by residual oligonucleotide cA (see text). (**B**) Inactivation of endogenous U7 RNA by targetting of RNase H with oligonucleotide cA. The samples from (A) (3 oocyte equivalents) were used in a primer extension with a primer (cBX) that yields a specific 33 nt extension product only with *Xenopus* U7 RNA. In lane 9 a band due to premature termination of reverse transcription is indicated with an asterisk.

RNA–protein contacts detectable by UV cross-linking are established in the cytoplasm

We next analysed the patterns of UV cross-linking in cytoplasmic extracts. All the RNA–protein adducts previously characterized for nuclear extracts, including the adduct between U7 Sm WT RNA and the 40 kDa protein, were also obtained with cytoplasmic extracts (Fig. 7). Of the three RNAs only U7 Sm MUT does not form any cross-links (lane 4). Moreover, a novel RNA–protein adduct which was not seen with nuclear samples is formed with U7 Sm WT (lane 2) and U7 Sm OPT RNA (lane 3, open arrowhead). The electrophoretic mobility of this adduct implies a protein moiety of 60–80 kDa. Further experiments indicated that all the cytoplasmic cross-linking products can be demonstrated in extracts taken 15 min after injection and persist for at least 18 h, whereas nuclear accumulation started at ~30 min for U7 Sm OPT and 3–6 h for U7 Sm WT RNA (data not shown).

In vitro synthesized U7 RNA is active in histone RNA processing

To determine if the particles assembled from *in vitro* transcribed U7 RNA are active in histone RNA processing we performed a triple injection experiment (32). First, endogenous U7 snRNAs were inactivated by nuclear injection of an oligodeoxynucleotide complementary to the 5′-end of *X.laevis* (and mouse) U7 snRNA (oligonucleotide cA; 22). This oligonucleotide targets the resident U7 RNA for degradation by RNase H, leading to a loss of histone RNA processing activity (6). This is demonstrated by a subsequent injection of a radiolabelled 85 nt long histone pre-mRNA from the mouse *H4-12* gene (12/12 RNA; 19; Fig. 1) as processing substrate. Untreated oocytes (Fig. 8A, lanes 2 and 9) or oocytes injected with an unrelated control oligonucleotide (lane 3) are able to cleave this substrate and produce a band of ~50 nt (49 plus the cap), corresponding to correctly processed histone RNA, whereas oocytes pre-injected with oligonucleotide cA alone fail to do so (lanes 4 and 10). Primer extension assays performed with the same RNA samples and a primer specific for *Xenopus* U7 RNA confirm that the endogenous U7 RNA has indeed been destroyed in those oocytes injected with oligonucleotide cA (Fig. 8B). Since oligodeoxynucleotides are degraded within a few hours in the oocyte (33), we injected *in vitro* transcribed and radioactively labelled (to monitor recovery) U7 Sm WT, U7 Sm MUT or U7 Sm OPT RNAs into the oocyte cytoplasm either 5 (Fig. 8A and B, left panel) or 24 h (right panel) after injection of oligonucleotide cA. The oocytes were then further incubated overnight to allow assembly and nuclear import of snRNPs. Thirdly, labelled and capped histone pre-mRNA was injected intranuclearly and after a further 2 h re-extracted and analysed to monitor the complementation of histone RNA 3′ processing caused by the injected U7 RNAs.

In this assay oligonucleotide cA-targeted oocytes complemented with U7 Sm WT RNA fully supported the processing

reaction (Fig. 8A, lanes 5 and 11), whereas the band corresponding to the processing product was not formed if U7 Sm WT alone but no histone pre-mRNA was injected into the oocytes (lane 8). As expected, U7 Sm MUT RNA, which does not enter the nucleus as a RNP particle, was inactive in complementation (lane 6). For U7 Sm OPT RNA no band corresponding to processed pre-mRNA could be observed when U7 Sm OPT RNA was injected 24 h after oligonucleotide cA (lane 12). When U7 Sm OPT RNA was injected 5 h after the oligonucleotide several faint bands were produced which migrated in the region of the expected processing product (lane 7). We later found that these bands were also produced if U7 Sm OPT alone but no histone pre-mRNA was injected (data not shown). This phenomenon is most likely related to the very rapid nuclear import of U7 Sm OPT RNA at a time when oligonucleotide cA has not yet been fully degraded. Most importantly, however, we conclude that *in vitro* synthesized U7 Sm WT RNA can assemble into a functional U7 snRNP. In contrast, both U7 Sm MUT and U7 Sm OPT RNA, albeit for different reasons, do not produce functional U7 snRNPs. Thus the injected *in vitro* synthesized U7 RNAs behave functionally like their counterparts transcribed *in vivo* from an injected genes (6).

Since U7 Sm WT RNA carrying an ApppG cap accumulates in the nucleus, we tested whether it can also function in histone RNA 3′ processing. After oligonucleotide cA targeted destruction of the resident *Xenopus* U7 snRNPs the oocytes were complemented with either m7G- or ApppG-capped U7 Sm WT RNA. In agreement with the above, U7-depleted oocytes complemented with m7G-capped U7 Sm WT RNA form the correct cleavage product of 12/12 RNA (lane 3), however, a weak additional band shorter by 1 or 2 nt is also obtained. This band is observed in some experiments and presumably results from exonucleolytic nibbling, once the original cleavage has occurred. Most importantly, the ApppG-capped U7 Sm WT RNA is also able to complement histone RNA processing (lane 4). However, in this case the shorter band prevails in intensity over the correct 50 nt product. U7-depleted oocytes injected with only substrate (lane 2) or only the U7 RNAs (lanes 5 and 6) do not form any bands of a similar size. In addition, in none of the samples injected with the antisense oligonucleotide could any intact *Xenopus* U7 RNA be detected by primer extension assay (Fig. 9B). Together with the finding that ApppG-capped transcripts cannot be immunoprecipitated by anti-3mG cap antibodies after injection into oocytes (Fig. 3A) these results indicate that the correct 3mG cap structure is not neccessary for U7 snRNP function, at least in *Xenopus* oocytes.

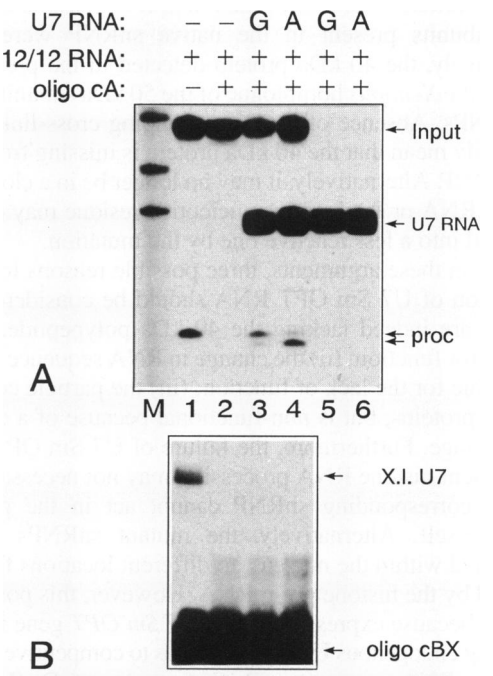

Figure 9. Complementation of histone pre-mRNA processing is independent of the cap structure present on U7 RNA. (**A**) Biochemical complementation of histone pre-mRNA processing with *in vitro* synthesized U7 RNAs. *In vitro* synthesized 7mG- or ApppG-capped U7 Sm WT RNAs were injected into the ooplasm of oocytes depleted of endogenous U7 RNAs by targeting with oligonucleotide cA 24 h previously. After 18 h incubation 12/12 histone pre-mRNA was injected into the nucleus of the same oocytes. After an additional 2 h total oocyte RNA was extracted and analysed on a denaturing polyacrylamide gel (2 oocyte equivalents/lane). Lane M, size marker (see Fig. 8); lane 1, processing by native oocytes; lane 2, (lack of) processing by oocytes depleted of U7 RNA with oligonucleotide cA; lane 3, complementation of processing by injection of 7mG-capped U7 Sm WT RNA; lane 4, complementation with ApppG-capped U7 Sm WT RNA; lane 5, as 3 but 12/12 RNA omitted; lane 6, as 4 but 12/12 RNA omitted. Migration of U7 RNAs and of the input and processing product of 12/12 histone pre-mRNA is indicated. The appearance of dual bands corresponding to the processing product (lanes 3 and 4) is seen in some experiments and may be due to exonucleolytic nibbling, once cleavage has occurred. (**B**) Inactivation of endogenous U7 RNA by targeting of RNase H with oligonucleotide cA. The samples from (A) (3 oocyte equivalents) were used in a primer extension with a primer (cBX) that yields a specific 33 nt extension product only with *Xenopus* U7 RNA.

DISCUSSION

In this paper we have studied the structure and function of U7 snRNPs by microinjection of synthetic U7 transcripts into *X.laevis* oocytes. Similar reconstitution studies using oocytes specifically depleted of U1 or U2 snRNPs by oligonucleotide-directed RNase H cleavage have provided important information about the structure and function of these spliceosomal snRNAs (32,34). However, in these cases complementation was only obtained with natural and not with *in vitro* transcribed U1 or U2 snRNAs. Complementation with synthetic RNA has, however, been achieved for the small nucleolar U8 RNA (35).

Comparison of functional and non-functional U7 snRNPs

One aim of this study was to investigate the difference between functional U7 Sm WT and non-functional U7 Sm OPT RNA, both of which form snRNPs. After assembly in the oocytes both RNAs can be cross-linked to two proteins of ~30 and 10 kDa respectively, which were identified as the common G and B/B′ polypeptides. Cross-linking of protein G to a similar location within the Sm binding site of U1 RNA has been described (29), but no other cross-linking of a snRNA to proteins B/B′ has been reported. The most notable structural difference between the two particles is that U7 Sm WT, but not U7 Sm OPT, RNA can be cross-linked to a 40 kDa protein (Fig. 4). This protein is larger than any of the described common snRNP proteins and hence is most likely a U7-specific polypeptide. Purification of mouse U7 snRNPs has not revealed a protein subunit of this size, but rather two U7-specific polypeptides of 50 and 14 kDa (4). Since the

purified particles were non-functional, it is possible that one or more subunits present in the native snRNP were missing. Alternatively, the 40 kDa protein detected in the present study could be the *Xenopus* homologue of the 50 kDa subunit of mouse U7 snRNPs. Absence of the corresponding cross-link does not necessarily mean that the 40 kDa protein is missing from U7 Sm OPT snRNP. Alternatively, it may no longer be in a close contact with the RNA or the reactive nucleotide residue may have been converted into a less reactive one by the mutation.

Based on these arguments, three possible reasons for the lack of function of U7 Sm OPT RNA should be considered: (i) the particles are indeed lacking the 40 kDa polypeptide, which is required for function; (ii) the change in RNA sequence is directly responsible for the lack of function; (iii) the particle contains all required proteins, but is non-functional because of a conformational change. Furthermore, the failure of U7 Sm OPT RNA to complement histone RNA processing may not necessarily mean that the corresponding snRNP cannot act in the processing reaction itself. Alternatively, the mutant snRNPs might be mistargeted within the nucleus, to different locations from those occupied by the histone pre-mRNA. However, this possibility is unlikely, because expression of the *U7 Sm OPT* gene in oocytes containing endogenous U7 snRNPs leads to competitive inhibition of histone RNA processing (B. Stefanovic and D. Schümperli, unpublished results) and because the Sm OPT sequence is also inactive in a *cis*-cleavage assay (36).

One binding site for common and U7-specific proteins?

A previous structure–function analysis of the sea urchin *U7* gene defined the Sm binding site within the sequence CAAGUUUCUCUAGA (2). All nucleotides located further 5′ could be deleted without losing Sm precipitability and the 3′ stem–loop could be replaced by unrelated sequences as long as a similar secondary structure could still be formed. This narrow definition of the Sm binding site contrasts with the situation encountered in spliceosomal snRNPs. Jarmolowski *et al.* (37) have shown that the Sm binding sites of *Xenopus* U1 and U5 RNAs are not interchangeable in promoting assembly with the common Sm proteins, although they are almost identical in sequence. From these and other observations they concluded that the Sm binding site, in combination with other structural elements located in the flanking stem–loops, specifies the correct assembly of a particular snRNA with Sm proteins. However, for U7 RNA the Sm binding site appears to play the dominant role in assembly with the common snRNP proteins.

The present study revealed that all three close RNA–protein contacts detectable by UV cross-linking are located within this sequence (Fig. 6). Unfortunately, the low efficiency of UV cross-linking achieved so far has precluded the identification of double or triple cross-linking products which would prove that all interactions occur within the same particle. Nevertheless, we consider it likely that the particles are homogeneous with respect to these protein contacts, since the three photoadducts have similar relative intensities in the cytoplasmic and nuclear fractions (Figs 4 and 7) and also accumulate proportionally over time in both kinds of extracts (data not shown).

It is most interesting that the apparently U7-specific 40 kDa protein also interacts with the Sm binding site. As far as has been analysed, the snRNP-specific proteins of other Sm-type snRNPs bind to structural features of the snRNA outside the Sm binding site (reviewed in 5). Paradigms for this kind of interaction are binding of the U1-specific proteins 70K and A to hairpins I and II of U1 snRNA. In these cases it was also shown conclusively that these proteins can bind to the RNA independently of other proteins and, in particular, of the Sm core (38–41). Other snRNP-specific proteins, such as the U1-specific protein C, may bind to their cognate snRNP via protein–protein interactions, presumably requiring the previous binding of at least one other snRNP-specific polypeptide (reviewed in 5). In contrast, the common proteins binding to the Sm site may form a similar structure in all snRNPs, as is indicated by the fact that they can form a 6S complex even in the absence of RNA (42). Therefore, U7 appears to be the first and perhaps only Sm-type snRNP in which both common and particle-specific proteins interact closely with the same short stretch of nucleotides. This peculiarity is reflected in the atypical sequence of the U7 Sm binding site, whose first half, AAUUUGU in mouse or AGUUUCU in sea urchin, may function more like a 'true' Sm binding site. The second half, CUAG, is specific for U7 RNA and appears to make contact with the 40 kDa protein. It is not known whether these two half-sites can function independently of each other. Several mutations of the corresponding region of sea urchin U7 RNA resulted in a loss of both Sm precipitability and snRNP function (2). The only mutant so far that retains Sm precipitability but leads to a loss of function and, perhaps, of binding of the 40 kDa protein is U7 Sm OPT. However, in this mutant both putative half-sites have been altered and the Sm site has deliberately been extended and optimized. Concerning the inverse, we have so far not been able to generate a mutant that would convincingly lose all interaction with the common Sm proteins and yet retain binding to the 40 kDa polypeptide (B. Stefanovic and D. S. Schümperli, unpublished results).

Mode of assembly and nuclear import of U7 snRNA

The cap structure of U7 RNA becomes hypermethylated *in vivo* (3) and the same is true for the injected *in vitro* sythesized U7 RNAs used in this study (Fig. 3A). We have therefore analysed whether this structure is required for assembly, nuclear accumulation or function of U7 snRNPs. Of these processes only nuclear import is detectably affected (Fig. 3B). However, a residual fraction of injected ApppG-capped U7 RNA can still be imported and is even functional in histone RNA processing (Fig. 9). Of the other snRNAs only U8 has been shown to function without a 3mG cap (35). Generally, cap hypermethylation is thought to occur after the Sm proteins have assembled with the RNA (31, reviewed in 43,44). In agreement with this, cap hypermethylation in U7 RNA is Sm-dependent. Regarding nuclear import, U7 RNA behaves more like U4 and U5 RNAs, where the 3mG cap is not absolutely required for nuclear accumulation but enhances the process (45), and unlike U1 and U2 snRNAs, where the binding of common Sm proteins and hypermethylation of the cap structure are two independent and neccessary nuclear targeting signals (45–48). However, these differences are only valid for *Xenopus* oocytes, since in mammalian tissue culture cells (49) and in an *in vitro* nuclear import system derived from such cells (50) hypermethylation of the cap structure is also dispensible for nuclear targeting of U1 and U2 snRNPs.

Interestingly, U7 Sm MUT RNA shows a low level of nuclear accumulation when bearing an ApppG cap, but is completely cytoplasmic with the m7G cap (Fig. 3). This result can be

explained if the free RNA bearing either cap structure can enter the nucleus by diffusion, but the normal m7G cap promotes a specific re-export which practically amounts to an exclusion from the nucleus. Alternatively, a cytoplasmic m7G cap binding protein might inhibit import of the m7G-capped U7 Sm MUT RNA. In either case a certain fraction of the ApppG-capped U7 Sm WT and U7 Sm OPT RNAs found in the nucleus could also be explained by this non-specific mechanism. However, because the proportion of nuclear RNA is higher for both of these RNAs than for the ApppG-capped U7 Sm MUT RNA, these RNAs must also be imported by a specific, Sm-dependent mechanism.

Cytoplasmic samples subjected to UV cross-linking, in addition to the cross-linking products found in nuclear fractions, also contain a cross-linking product suggestive of a 60–80 kDa protein (Fig. 7). This adduct is visible at very early time points and remains almost constant over time (data not shown). Using the same mapping technique as in Figure 6 we have located this cross-link to the stretch of U residues at positions 15–18 (Fig. 1; data not shown). This region of U7 RNA participates in base pairing to the histone pre-mRNA during histone RNA 3′ processing (8,13,22). The identity of this cytoplasmic RNA binding protein is not known. One possibility is that it is involved in nuclear import of U7 snRNPs.

Finally, cross-linking of the apparently U7-specific 40 kDa protein in cytoplasmic extracts may represent a further difference between U7 and the other Sm-type snRNPs. For the other snRNPs the location in the cell where the particle-specific proteins associate with their respective snRNP particles is not known. However, it has been shown that binding of the U1-specific proteins A, C and 70K is not required for nuclear import of U1 RNA (47). Moreover, the U1- and U2-specific snRNP proteins can enter the nucleus independently of their respective core RNP (51). Thus it is likely that the addition of snRNP-specific proteins is normally a nuclear event. The fact that the 40 kDa protein (and perhaps other U7-specific proteins as well) associates with U7 RNA in the cytoplasm raises the interesting possibility that U7 snRNPs might be competent for histone RNA cleavage before entering the nucleus.

ACKNOWLEDGEMENTS

We thank T. Wyler and T. Murri for taking good care of the frogs, D. Soldati for constructing plasmid OT7U7, H. Brigger and T. Wyler for preparing photographs, W. -D. Heyer for antibodies and B. Müller and W. -D. Heyer for helpful criticism of the manuscript. We acknowledge financial support by the State of Bern and by grant 3100-27753.89 from the Swiss National Science Foundation to D.S. and by the Deutsche Forschungsgemeinschaft (SFB 272/A3) to R.L. B.S. was in part supported by a post-doctoral fellowship from the Roche Research Foundation.

REFERENCES

1 Galli,G., Hofstetter,H., Stunnenberg,H.G. and Birnstiel,M.L. (1983) *Cell*, **34**, 823–828.
2 Gilmartin,G.M., Schaufele,F., Schaffner,G. and Birnstiel,M.L. (1988) *Mol. Cell. Biol.*, **8**, 1076–1084.
3 Strub,K. and Birnstiel,M.L. (1986) *EMBO J.*, **5**, 1675–1682.
4 Smith,H.O., Tabiti,K., Schaffner,G., Soldati,D., Albrecht,U. and Birnstiel,M.L. (1991) *Proc. Natl. Acad. Sci. USA*, **88**, 9784–9788.
5 Lührmann,R., Kastner,B. and Bach,M. (1990) *Biochim. Biophys. Acta*, **1087**, 265–292.
6 Grimm,C., Stefanovic,B. and Schümperli,D. (1993) *EMBO J.*, **12**, 1229–1238.
7 Reddy,R. and Busch,H. (1988) In Birnstiel,M.L. (ed.), *Structure and Function of Major and Minor Small Nuclear Ribonucleoprotein Particles.* Springer-Verlag, Berlin, Germany, pp. 1–37.
8 Bond,U.M., Yario,T.A. and Steitz,J.A. (1991) *Genes Dev.*, 5, 1709–1722.
9 Schaufele,F., Gilmartin,G.M., Bannwarth,W. and Birnstiel,M.L. (1986) *Nature*, **323**, 777–781.
10 Melin,L., Soldati,D., Mital,R., Streit,A. and Schümperli,D. (1992) *EMBO J.*, **11**, 691–697.
11 Birnstiel,M.L. and Schaufele,F.J. (1988) In Birnstiel,M.L. (ed.), *Structure and Function of Major and Minor Small Nuclear Ribonucleoprotein Particles.* Springer-Verlag, Berlin, Germany, pp. 155–182.
12 De Lorenzi,M., Rohrer,U. and Birnstiel,M.L. (1986) *Proc. Natl. Acad. Sci. USA*, **83**, 3243–3247.
13 Mowry,K.L. and Steitz,J.A. (1987) *Science*, **238**, 1682–1687.
14 Gruber,A., Soldati,D., Burri,M. and Schümperli,D. (1991) *Biochim. Biophys. Acta*, **1088**, 151–154.
15 Phillips,S.C. and Turner,P.C. (1991) *Nucleic Acids Res.*, **19**, 1344.
16 Phillips,S.C. and Birnstiel,M.L. (1992) *Biochem. Biophys. Acta*, **1131**, 95–98.
17 Kunkel,T.A. (1985) *Proc. Natl. Acad. Sci. USA*, **82**, 488–492.
18 Kunkel,T.A., Roberts,J.D. and Zakour,R.A. (1987) *Methods Enzymol.*, **154**, 367–382.
19 Streit,A., Wittop Koning,T., Soldati,D., Melin,L. and Schümperli,D. (1993) *Nucleic Acids Res.*, **21**, 1569–1575.
20 Sanger,F., Nicklen,S. and Coulson,A.R. (1977) *Proc. Natl. Acad. Sci. USA*, **74**, 5463–5467.
21 England,T.E. and Uhlenbeck,O.C. (1978) *Nature*, **275**, 560–561.
22 Soldati,D. and Schümperli,D. (1988) *Mol. Cell. Biol.*, **8**, 1518–1524.
23 Lund,E. and Dahlberg,J.E. (1989) *EMBO J.*, **8**, 287–292.
24 Dignam,J.D., Lebovitz,R.M. and Roeder,R.G. (1983) *Nucleic Acids Res.*, **11**, 1475–1489.
25 Mital,R., Albrecht,U. and Schümperli,D. (1993) *Nucleic Acids Res.*, **21**, 1049–1050.
26 Laemmli,U.K. (1970) *Nature*, **227**, 680–685.
27 Lerner,E.A., Lerner,M.R., Janeway,C.A. and Steitz,J.A. (1981) *Proc. Natl. Acad. Sci. USA*, **78**, 2737–2741.
28 Lührmann,R., Appel,B., Bringmann,P., Rinke,J., Reuter,R., Rothe,S. and Bald,R. (1982) *Nucleic Acids Res.*, **10**, 7103–7113.
29 Heinrichs,V., Hackl,W. and Lührmann,R. (1992) *J. Mol. Biol.*, **227**, 15–28.
30 Reuter,R. and Lührmann, R.(1986) *Proc. Natl. Acad. Sci. USA*, **83**, 8689–8693.
31 Mattaj, I.W. (1986) *Cell*, **46**, 905–911.
32 Pan,Z.Q. and Prives,C. (1988) *Science*, **241**, 1328–1331.
33 Cazenave,C., Chevrier,M., Thuong,N.T. and Hélène,C. (1987) *Nucleic Acids Res.*, **24**, 10507–10521.
34 Hamm,J., Dathan,N.A. and Mattaj,I.W. (1989) *Cell*, **53**, 159–169.
35 Peculis,B.A. and Steitz,J.A. (1994) *Genes Dev.*, **8**, 2241–2255.
36 Stefanovic,B, Wittop Koning,T.H. and Schümperli,D. (1995) *Nucleic Acids Res.*, **23**, 3152–3160.
37 Jarmolowski,A. and Mattaj,I.W. (1993) *EMBO J.*, **12**, 223–232.
38 Lutz-Reyermuth,C. and Keene,J.D. (1989) *Mol. Cell. Biol.*, **9**, 2975–2982.
39 Patton,J.R., Habets,W., Van Venrooij,W.J. and Pederson.,T. (1989) *Mol. Cell. Biol.*, **9**, 3360–3368.
40 Query,C.C., Bentley,R.C. and Keene,J.D. (1989) *Mol. Cell. Biol.*, **9**, 4872–4881.
41 Surowy,C.S., Van Santen,V.L., Scheib-Wixted,S.M. and Spritz,R.A. (1989) *Mol. Cell. Biol.*, **9**, 4179–4186.
42 Fisher,D.E., Conner,G.E., Reeves,W.H., Wisniewolski,R. and Blobel,G. (1985) *Cell*, **42**, 751–758.
43 Mattaj,I.W. (1988) In Birnstiel,M.L. (ed.), *Structure and Function of Major and Minor Small Nuclear Ribonucleoprotein Particles.* Springer-Verlag, Berlin, Germany, pp. 100–114.
44 Nigg,E.A., Baeuerle,P.A. and Lührmann,R. (1991) *Cell*, **66**, 15–22.
45 Fischer,U., Darzynkiewicz,E., Tahara,S.M., Dathan,N.A., Lührmann,R. and Mattaj,I.W. (1991) *J. Cell Biol.*, **113**, 705–714.
46 Fischer,U. and Lührmann,R. (1990) *Science*, **249**, 786–790.
47 Hamm,J., Darzynkiewicz,E., Tahara,S.M. and Mattaj,I.W. (1990) *Cell*, **62**, 569–577.
48 Michaud,N. and Goldfarb,D. (1992) *J. Cell Biol.*, **116**, 851–861.
49 Fischer,U., Heinrich,J., van Zee,K., Fanning,E. and Lührmann,R. (1994) *J. Cell Biol.*, **125**, 971–980.
50 Marshallsay,C. and Lührmann,R. (1994) *EMBO J.*, **13**, 222–231.
51 Feeney,R.J. and Zieve,G.W. (1990) *J. Cell Biol.*, **110**, 871–881.